

# Event-triggered neural network control of autonomous surface vehicles over wireless network

Mingao LV<sup>1</sup>, Dan WANG<sup>1\*</sup>, Zhouhua PENG<sup>1\*</sup>, Lu LIU<sup>1</sup> & Haoliang WANG<sup>2</sup>

<sup>1</sup>*School of Marine Electrical Engineering, Dalian Maritime University, Dalian 116026, China;*

<sup>2</sup>*School of Marine Engineering, Dalian Maritime University, Dalian 116026, China*

Received 10 May 2019/Accepted 16 September 2019/Published online 16 March 2020

**Abstract** In this paper, an event-triggered neural network control method is proposed for autonomous surface vehicles subject to uncertainties and input constraints over wireless network. An event-triggered mechanism with three logic rules is employed to determine the wireless data transmission of states and control inputs. An event-driven neural network is applied to approximate the uncertainties using aperiodic sampled states. In addition, a predictor is employed to update the weights of neural network. An event-based bounded kinetic control law is applied to address the actuator constraints. The advantage of the proposed event-triggered neural network control approach is that the network traffic can be reduced while guaranteeing system stability and speed following performance. The closed-loop control system is proved to be input-to-state stable via cascade theory. The Zeno behavior can be avoided via the proposed event-triggered neural network control approach. A simulation example is provided to demonstrate the effectiveness of the proposed event-triggered neural network control approach for autonomous surface vehicles.

**Keywords** event-triggered control, aperiodic sampling, autonomous surface vehicles, neural network, actuator constraint

**Citation** Lv M G, Wang D, Peng Z H, et al. Event-triggered neural network control of autonomous surface vehicles over wireless network. *Sci China Inf Sci*, 2020, 63(5): 150205, <https://doi.org/10.1007/s11432-019-2679-5>

## 1 Introduction

In the past decades, motion control problems of autonomous surface vehicles (ASVs) have attracted great attention by numerous researchers [1,2]. Kinematic and kinetic controls are two fundamental problems in motion control of ASVs. Specifically, the kinematic control occupies a pivotal role in trajectory tracking, and the kinetic control plays a crucial role in driving ASVs to achieve a desired velocity. In the kinetic of ASVs, there are some uncertainties caused by unmodelled dynamics, uncertain model parameters and external disturbance [1,2]. This brings challenges to controller design.

To solve the effects of uncertainties, a quantity of control approaches have been presented from papers [3–24]. In [3–11], neural networks (NNs) were used to approximate the uncertainties. In [12–15], nonlinear disturbance observers were employed to approximate the uncertainties caused by unknown external disturbances. In [16–18], sliding model controls were developed to reduce the effects caused by external disturbances. In [19,20], fuzzy logic systems were employed to estimate the lumped unknown functions. In [21–24], adaptive techniques were used to reject the model uncertainties and compensate the effects of external disturbances. Nevertheless, the above systems work with periodic sampling and controlling in these studies [3–24], known as periodic-triggered control systems. To guarantee the stability

\* Corresponding author (email: [dwangdl@gmail.com](mailto:dwangdl@gmail.com), [zhpeng@dlnu.edu.cn](mailto:zhpeng@dlnu.edu.cn))

and desired control performance, the periods of sampling and controlling are usually small, which will cause a mass of data transmission and update.

Unlike the above control methods, an aperiodic control technique called event-triggered control is presented in recent years [25–32]. The sampling and controlling of the systems only occur when the predefined events are true in event-triggered controls, such that the two-way data transmissions can be reduced. It takes advantages in reducing expense on communication resources, and thus has wide application prospect in networked control systems. To reduce the network traffic, several event-triggered control approaches have been developed in [25–32]. In [25, 27], event-triggered adaptive control methods were introduced to schedule data exchange dependent upon errors exceeding user-defined thresholds to reduce wireless network utilization. In [26], an approximation-based event-triggered control method was proposed for multi-input multi-output uncertain nonlinear continuous-time systems in affine form. In [28], an event-triggered model predictive control method was proposed for continuous-time nonlinear systems. In [29], a periodically event-triggered control method was introduced for linear systems to reduce the number of transmissions. In [30], an observer-type event-triggered control protocol was proposed to determine data transmissions. In [31], asynchronous event-triggered control algorithms were proposed based on the triggering time sequences of all agents. In [32], a layered event-triggered consensus scheme was proposed for multiagent systems with a multilayer structure. However, the event-triggered methods are rarely applied on the control of ASVs.

Constraints widely exist in practical systems [3, 13, 14, 33–37]. The limited inputs of the motor and rudder of ASV may cause the input constraints. In the controller design, ignoring constraints may reduce system performance and controllability, and even result in instability in some cases. Hence, taking constraints into consideration is necessary in practical systems. A number of methods were proposed to solve the constraint problems of ASVs [3, 13, 34–37]. In [3, 34], bounded feedback controllers were proposed to solve input constraints. In [13, 35, 36], auxiliary systems were introduced to make compensation for the saturation constraints of inputs. In [37], a smooth function was applied to deal with the input saturated function.

Motivated by the studies above, this study takes uncertainties and input constraints into consideration in the speed tracking problem of ASVs. An event-driven NN is employed to approximate the uncertainties caused by unmodelled dynamics, external disturbance and uncertain model parameters. An event-based bounded kinetic control law is employed to solve the input constraints. A predefined threshold-based event-triggered mechanism is employed to determine the network transmissions. With the event-triggered mechanism, the data transmissions between the controller and the ASV are aperiodic. The advantage of the proposed approach is that the network traffic can be degraded while ensuring the system stability and control performance. A simulation example is provided to illustrate the effectiveness of the presented event-triggered NN control method.

Compared with previous studies in [2–11, 15–17, 19, 22, 25, 26], the contributions of this paper are summarized below. Firstly, compared with the NN control approaches proposed in [3–9, 11], where the systems work with fixed sampling and controlling period, the proposed control method updates the vehicle states and control inputs aperiodically. Network transmissions occur only at triggering instants. The instants are determined by the proposed event-triggered mechanism to degrade the network traffic. Secondly, compared with the control methods presented in [2, 16, 17, 19, 22, 25], where the input constraints of ASV are neglected, the proposed method takes input constraints into consideration and presents a saturated kinetic control law. The outputs of the controller are bounded, and the bound is known as a priori by employing a saturated function and a projection operator. Thirdly, compared with the presented controllers in [10, 26], where the estimation and control are coupled, the proposed controller is formed with estimation subsystem and kinetic control subsystem. Thus, it is flexible to combine the estimation method with other control methods. The resulting closed-loop control system is proved to be input-to-state stable, and all error signals are proved to be uniformly ultimately bounded via Lyapunov analysis.

The rest paper is organized as follows. Preliminaries and problem formulation are stated in Section 2. The approximation of uncertainties, saturated kinetic control law design, event-triggered mechanism and

zero order holds (ZOHs) are presented in Section 3. The stability of the resulting closed-loop control system and Zeno behavior are analyzed in Section 4. An illustration of simulation is shown in Section 5. The conclusion is given in Section 6.

## 2 Preliminaries and problem formulation

### 2.1 Preliminaries

(1) Notation: Throughout this paper,  $\mathbb{N}$  denotes non-negative integer set.  $\mathbb{R}, \mathbb{R}^+, \mathbb{R}^n, \mathbb{R}^{n+}, \mathbb{R}^{n \times m}$  denote real set, positive real set,  $n \times 1$ -dimensional column vectors,  $n \times 1$ -dimensional positive column vectors, the  $n \times m$ -dimensional real matrices, respectively.  $(\cdot)^T$  denotes transform.  $\|\cdot\|_F$  denotes Frobenius norm.  $|\cdot|$  denotes absolute values.  $\|\cdot\|$  denotes 2-norm.  $\text{diag}\{a_i\}$  denotes a block-diagonal matrix, where  $a_i$  is the  $i$ th diagonal element.  $\lambda_{\max}(A)$  and  $\lambda_{\min}(A)$  are the maximal and minimal eigenvalue of a matrix  $A$ , respectively.  $\bar{A}$  denotes the “not A” logic operator.  $\wedge$  denotes the “and” logic operator.

(2) NN: For a given continuous function  $f(\rho) : \mathbb{R}^n \rightarrow \mathbb{R}$ , it can be approximated by an NN with an ideal constant weight  $W \in \mathbb{R}^n$  and a known activation function  $\beta(\rho) \in \mathbb{R}^n$  as [6]

$$f(\rho) = W^T \beta(\rho) + \varepsilon_f(\rho), \quad \rho \in \Omega, \quad (1)$$

where  $\Omega$  denotes a compact set, and  $\varepsilon_f(\rho)$  denotes the approximation error. There exist positive constants  $W^* \in \mathbb{R}^+$ ,  $\beta^* \in \mathbb{R}^+$  and  $\varepsilon_f^* \in \mathbb{R}^+$  such that  $\|W\|_F \leq W^*$ ,  $\|\beta(\rho)\| \leq \beta^*$  and  $\|\varepsilon_f(\rho)\| \leq \varepsilon_f^*$ .

(3) Projection operator: Let  $\varrho : \mathbb{R}^n \rightarrow \mathbb{R}$  denote a continuously differentiable convex function. It is given by  $\varrho(\zeta) \triangleq (\zeta^T \zeta - \zeta_o^2) / (2\varepsilon_\zeta \zeta_o^2 + \varepsilon_\zeta^2)$  with  $\zeta \in \mathbb{R}^n$ , where  $\varepsilon_\zeta \in \mathbb{R}^+$  denotes a projection tolerance bound, and  $\zeta_o \in \mathbb{R}$  denotes a projection norm bound. The projection operator  $\text{Proj} : \mathbb{R}^n \times \mathbb{R}^n \rightarrow \mathbb{R}^n$  is defined as [38]

$$\text{Proj}(\zeta, \xi) \triangleq \begin{cases} \xi, & \text{if } \varrho(\zeta) < 0, \\ \xi, & \text{if } \varrho(\zeta) \geq 0 \wedge \nabla \varrho(\zeta) \xi \leq 0, \\ \xi - \frac{(\nabla \varrho(\zeta))^T \nabla \varrho(\zeta)}{\|\nabla \varrho(\zeta)\|^2} \xi \varrho(\zeta), & \text{if } \varrho(\zeta) \geq 0 \wedge \nabla \varrho(\zeta) \xi > 0, \end{cases} \quad (2)$$

where  $\xi \in \mathbb{R}^n$  and  $\nabla \varrho(\zeta) = [\partial \varrho(\zeta) / \zeta_1, \dots, \partial \varrho(\zeta) / \zeta_N]^T$ . According to the definition of the projection operator, it renders

$$(\zeta - \zeta^*)^T (\text{Proj}(\zeta, \xi) - \xi) \leq 0, \quad (3)$$

where  $\zeta^* \in \mathbb{R}^n$  denotes the true value of the parameter  $\zeta$ .

### 2.2 Problem formulation

According to [1], the kinematics of ASVs as shown in Figure 1 can be expressed by

$$\dot{\eta} = J(\psi)\nu, \quad (4)$$

where  $\eta = [x, y, \psi]^T \in \mathbb{R}^3$  denotes the earth-fixed position  $(x, y)$  and heading  $\psi$ ;  $J(\psi) \in \mathbb{R}^{3 \times 3}$  is the transformation matrix between the body-fixed and earth-fixed reference frame;  $\nu = [u, v, r]^T \in \mathbb{R}^3$  denotes the surge, sway and angular velocity in body-fixed frame.

The kinetics of ASVs can be represented by [1]

$$M\dot{\nu} = \tau_s - C(\nu)\nu - D(\nu)\nu + g(\nu, \eta) + \tau_w(t), \quad (5)$$

with

$$J(\psi) = \begin{bmatrix} j_{11} & j_{12} & 0 \\ j_{21} & j_{22} & 0 \\ 0 & 0 & j_{33} \end{bmatrix}, \quad M = \begin{bmatrix} m_{11} & 0 & 0 \\ 0 & m_{22} & m_{23} \\ 0 & m_{32} & m_{33} \end{bmatrix}, \quad C(\nu) = \begin{bmatrix} 0 & 0 & c_{13} \\ 0 & 0 & c_{23} \\ c_{31} & c_{32} & 0 \end{bmatrix}, \quad D(\nu) = \begin{bmatrix} d_{11} & 0 & 0 \\ 0 & d_{22} & d_{23} \\ 0 & d_{32} & d_{33} \end{bmatrix},$$

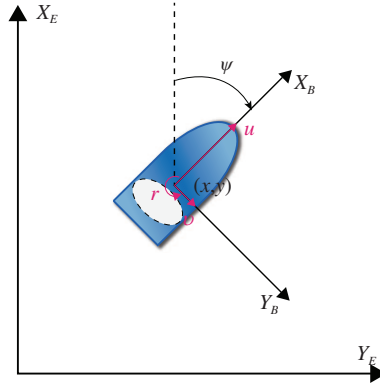


**Figure 1** (Color online) Reference frames.

$$\begin{aligned} j_{11} &= \cos(\psi), & j_{22} &= \cos(\psi), & j_{33} &= 1, & j_{12} &= -\sin(\psi), & j_{21} &= \sin(\psi), \\ c_{13} &= -m_{22}\nu - 0.6m_{23} - 0.6m_{32}, & c_{23} &= m_{11}u, & c_{31} &= -c_{13}, & c_{32} &= -c_{23}, \end{aligned}$$

where  $M = M^T \in \mathbb{R}^{3 \times 3}$  is a known inertial matrix;  $C(\nu) = -C(\nu) \in \mathbb{R}^{3 \times 3}$  is a centrifugal and coriolis matrix;  $\tau_s = [\tau_{us}, \tau_{vs}, \tau_{rs}]^T \in \mathbb{R}^3$  denotes the control inputs for the ASV;  $D(\nu) \in \mathbb{R}^{3 \times 3}$  is a hydrodynamic damping matrix;  $g(\nu, \eta)$  represents the unmodeled dynamics including gravitational/buoyancy forces and moments;  $\tau_w = [\tau_{wu}, \tau_{wv}, \tau_{wr}]^T \in \mathbb{R}^3$  denotes the bounded environmental forces.

In reality, the control input  $\tau_s$  of the vehicle kinetics is constrained. Let the upper bound of constrained control input be  $\tau_{s \max} = [\tau_{us \max}, \tau_{vs \max}, \tau_{rs \max}]^T \in \mathbb{R}^{3+}$ , and the lower bound be  $\tau_{s \min} = [\tau_{us \min}, \tau_{vs \min}, \tau_{rs \min}]^T \in \mathbb{R}^{3+}$ . The input constrain can be expressed as  $-\tau_{s \min} \leq \tau_s \leq \tau_{s \max}$ .

The objective is to develop an event-triggered NN control method for the ASV with uncertainties and input constraints to follow a given speed command. The speed command could be any guidance signals generated by guidance systems at the kinematic level. The network traffic can be reduced by the proposed method while guaranteeing the system performance and stability.

### 3 Saturated kinetic control law and event-triggered mechanism design

In this section, the estimation of ASV uncertainties, the kinetic control law and the event-triggered mechanism are developed.

#### 3.1 Estimation of uncertainties

The ASV kinetics (4) can be rewritten as

$$M\dot{\nu} = \tau_s + f(\cdot), \quad (6)$$

where  $f(\cdot) = \tau_w(t) - C(\nu)\nu + g(\nu, \eta) - D(\nu)\nu$ . The unknown function  $f(\cdot) = [f_u(\cdot), f_v(\cdot), f_r(\cdot)]^T \in \mathbb{R}^3$  contains unmodelled dynamics, uncertain model parameters and external disturbance. Here, NN is applied to approximate the unknown function  $f(\cdot)$ .

Moreover, recalling the NN function (1),  $f_u(\cdot)$  in  $f(\cdot)$  can be expressed by using event-based state  $\vartheta_{us}$  as [26]

$$\begin{aligned} f_u(\cdot) &= W_u^T \beta(\vartheta_u) + \varepsilon_1(\vartheta_u), \\ &= W_u^T \beta(\vartheta_u) - W_u^T \beta(\vartheta_{us}) + W_u^T \beta(\vartheta_{us}) + \varepsilon_1(\vartheta_u), \\ &= W_u^T \beta(\vartheta_{us}) + W_u^T [\beta(\vartheta_u) - \beta(\vartheta_{us})] + \varepsilon_1(\vartheta_u), \\ &= W_u^T \beta(\vartheta_{us}) + \varepsilon_{e1}(\vartheta_{us}, e_{fu}), \end{aligned} \quad (7)$$

where  $\varepsilon_{e1}(\vartheta_{us}, e_{fu}) = W_u^T [\beta(\vartheta_{us} + e_{fu}) - \beta(\vartheta_{us})] + \varepsilon(\vartheta_{us} + e_{fu})$ , and  $\vartheta_{us}$  is given in (9).  $f_v(\cdot)$  and  $f_r(\cdot)$  are similar to  $f_u(\cdot)$ .

Similar to [26], given bounded weights  $W_u$ ,  $W_v$  and  $W_r \in \mathbb{R}^n$ , and  $\varepsilon_{ei}^* > 0$  for  $i = 1, 2, 3$ , the unknown function  $f(\cdot)$  is approximated by using NN as

$$\begin{cases} f_u(\cdot) = W_u^T \beta(\vartheta_{us}) + \varepsilon_{e1}(\vartheta_{us}, e_{fu}), \\ f_v(\cdot) = W_v^T \beta(\vartheta_{vs}) + \varepsilon_{e2}(\vartheta_{vs}, e_{fv}), \\ f_r(\cdot) = W_r^T \beta(\vartheta_{rs}) + \varepsilon_{e3}(\vartheta_{rs}, e_{fr}), \end{cases} \quad (8)$$

where

$$\begin{cases} \vartheta_{us} = [1, u_s(t) - u_s(t - t_p^*), \tau_{us}(t)]^T, \\ \vartheta_{vs} = [1, v_s(t) - v_s(t - t_p^*), \tau_{vs}(t)]^T, \\ \vartheta_{rs} = [1, r_s(t) - r_s(t - t_p^*), \tau_{rs}(t)]^T \end{cases} \quad (9)$$

are input vectors;  $u_s$ ,  $v_s$  and  $r_s$  are sampled vehicle states;  $t_p^*$  represents the sample period;  $\beta(\cdot)$  represents the bounded activation function;  $\varepsilon_{ei}(\cdot, \cdot)$  represents the event-driven NN reconstruction error;  $\varepsilon_e = [\varepsilon_{e1}, \varepsilon_{e2}, \varepsilon_{e3}]^T \in \mathbb{R}^3$  satisfies  $|\varepsilon_{ei}| \leq \varepsilon_{ei}^*$ ;  $e_{fu} = \vartheta_u - \vartheta_{us}$ ,  $e_{fv} = \vartheta_v - \vartheta_{vs}$  and  $e_{fr} = \vartheta_r - \vartheta_{rs}$  are event triggering errors, where

$$\begin{cases} \vartheta_u = [1, u(t) - u(t - t_p^*), \tau_u(t)]^T, \\ \vartheta_v = [1, v(t) - v(t - t_p^*), \tau_v(t)]^T, \\ \vartheta_r = [1, r(t) - r(t - t_p^*), \tau_r(t)]^T \end{cases} \quad (10)$$

are the input vectors of the NN function (1) without event-driven.

Using  $\hat{\nu} = [\hat{u}, \hat{v}, \hat{r}]^T \in \mathbb{R}^3$  to denote the estimate of  $\nu$ . To update the weights of NN, a predictor is applied for the vehicle kinetics (6) as

$$M\dot{\hat{\nu}} = -F(\hat{\nu} - \nu_s) + \tau_a + \tau_s, \quad (11)$$

where  $\tau_a = [\hat{W}_u^T \beta(\vartheta_{us}), \hat{W}_v^T \beta(\vartheta_{vs}), \hat{W}_r^T \beta(\vartheta_{rs})]^T \in \mathbb{R}^3$ ;  $F = \text{diag}\{k_1, k_2, k_3\} \in \mathbb{R}^{3 \times 3}$  with  $k_1, k_2$ , and  $k_3 \in \mathbb{R}^+$  being positive constants is a control gain matrix;  $\hat{W}_u, \hat{W}_v, \hat{W}_r$  are estimates of  $W_u, W_v, W_r$ , respectively.

The update laws for  $\hat{W}_u, \hat{W}_v, \hat{W}_r$  are designed as

$$\begin{cases} \dot{\hat{W}}_u(t) = -\Gamma_u \text{Proj}[\hat{W}_u(t), \beta(\vartheta_{us})(\hat{u} - u_s)], \\ \dot{\hat{W}}_v(t) = -\Gamma_v \text{Proj}[\hat{W}_v(t), \beta(\vartheta_{vs})(\hat{v} - v_s)], \\ \dot{\hat{W}}_r(t) = -\Gamma_r \text{Proj}[\hat{W}_r(t), \beta(\vartheta_{rs})(\hat{r} - r_s)], \end{cases} \quad (12)$$

where  $\Gamma_u, \Gamma_v$  and  $\Gamma_r \in \mathbb{R}^+$  denote adaptation gains. According to [38], the projection operation guarantees that there exist positive constants  $W_u^*, W_v^*, W_r^*, \varepsilon_1, \varepsilon_2$  and  $\varepsilon_3 \in \mathbb{R}^+$  satisfying

$$\begin{cases} \|\hat{W}_u(t)\| \leq \varepsilon_1 + W_u^*, \\ \|\hat{W}_v(t)\| \leq \varepsilon_2 + W_v^*, \\ \|\hat{W}_r(t)\| \leq \varepsilon_3 + W_r^*. \end{cases} \quad (13)$$

Let  $\tilde{W}_v = \hat{W}_v - W_v$ ,  $\tilde{W}_r = \hat{W}_r - W_r$  and  $\tilde{W}_u = \hat{W}_u - W_u$  denote the NN weights estimation errors. Let  $\tilde{\nu} = \hat{\nu} - \nu$  denote the state estimation error. Let  $\tilde{\nu}_s = \hat{\nu} - \nu_s$  denote the velocity estimation error after sampled, and  $\tilde{\nu}_e = \nu - \nu_s$  denote the event triggering error of vehicle states.

As a result, the error dynamics are given below:

$$\begin{cases} M\dot{\tilde{\nu}} = -F\tilde{\nu}_s + \tilde{\tau}_a - \varepsilon_e \\ \quad = -F\tilde{\nu} - F\tilde{\nu}_e + \tilde{\tau}_a - \varepsilon_e, \\ \dot{\tilde{W}}_u = -\Gamma_u \text{Proj}[\hat{W}_u, \beta(\vartheta_{us})(\tilde{u} + \tilde{\nu}_e)], \\ \dot{\tilde{W}}_v = -\Gamma_v \text{Proj}[\hat{W}_v, \beta(\vartheta_{vs})(\tilde{v} + \tilde{\nu}_e)], \\ \dot{\tilde{W}}_r = -\Gamma_r \text{Proj}[\hat{W}_r, \beta(\vartheta_{rs})(\tilde{r} + \tilde{\nu}_e)], \end{cases} \quad (14)$$

where  $\tilde{\tau}_a = [\tilde{W}_u^T \beta(\vartheta_{us}), \tilde{W}_v^T \beta(\vartheta_{vs}), \tilde{W}_r^T \beta(\vartheta_{rs})]^T$ .

### 3.2 Kinetic control law design

The desired velocity is represented by  $\nu_r$ . Use  $e = \nu - \nu_r$  to denote a velocity tracking error and  $\hat{e} = \hat{\nu} - \nu_r$  to denote an estimated velocity tracking error. Taking the time derivative and using (11),  $\dot{\hat{e}}$  is given by

$$M\dot{\hat{e}} = \tau_s + \tau_a - F(\hat{\nu} - \nu_s). \quad (15)$$

Then, a saturated kinetic control law is applied to stabilize  $\hat{e}$  as

$$\tau = -\frac{K\hat{e}}{\sqrt{\|\hat{e}\|^2 + \Delta^2}} - \tau_a, \quad (16)$$

where  $\tau = [\tau_u, \tau_v, \tau_r]^T \in \mathbb{R}^3$  denotes the outputs vector of the designed controller;  $\Delta \in \mathbb{R}^+$  is a positive constant;  $K = \text{diag}\{k_4, k_5, k_6\} \in \mathbb{R}^{3 \times 3}$  is a gain matrix with  $k_4, k_5$  and  $k_6 \in \mathbb{R}^+$  being positive constants.

Note that the control input of the ASV is  $\tau_s$ , and the output of the controller is  $\tau$ .  $\tau_s$  equals to  $\tau$  only at the triggering instants, which will be analyzed in Subsection 3.3. Let  $\tilde{\tau}_e = \tau - \tau_s$  denote the event triggering error of system control input. Substituting (16) into (15) and using  $\tilde{\nu} = \hat{\nu} - \nu$  and  $\tilde{\nu}_e = \nu - \nu_s$ , it leads to

$$\begin{aligned} M\dot{\hat{e}} &= -\frac{K\hat{e}}{\sqrt{\|\hat{e}\|^2 + \Delta^2}} - \tilde{\tau}_e - F(\hat{\nu} - \nu + \nu - \nu_s) \\ &= -\frac{K\hat{e}}{\sqrt{\|\hat{e}\|^2 + \Delta^2}} - \tilde{\tau}_e - F\tilde{\nu} - F\tilde{\nu}_e. \end{aligned} \quad (17)$$

A main feature of the proposed kinetic control law (16) is that the output  $\tau$  is bounded. The bound of  $\tau$  is known to a designer. With the condition

$$\frac{\|\hat{e}\|}{\sqrt{\|\hat{e}\|^2 + \Delta^2}} < 1, \quad (18)$$

it follows that

$$\|\tau\| \leq K^* + (W^* + \epsilon)\beta^*, \quad (19)$$

where  $\|K\|_F \leq K^*$  with  $K^* \in \mathbb{R}^+$ , and  $\epsilon \in \mathbb{R}^+$  is a positive constant.

### 3.3 Event-triggered mechanism design

In this subsection, an event-triggered mechanism is employed to reduce the network traffic. With the mechanism, the sampling and controlling of the systems only occur when the predefined events are true, such that the two-way data transmissions can be reduced. Three logic rules with predefined thresholds are designed in the mechanism. To be specific, define a state threshold  $\varepsilon_\nu = [\varepsilon_{\nu u}, \varepsilon_{\nu v}, \varepsilon_{\nu r}]^T \in \mathbb{R}^{3+}$  to determine whether to transmit the vehicle states, and a controller threshold  $\varepsilon_\tau = [\varepsilon_{\tau u}, \varepsilon_{\tau v}, \varepsilon_{\tau r}]^T \in \mathbb{R}^{3+}$  to determine whether to transmit the control inputs. The logic rules are defined as [27]

$$R_1 : \|\nu_s(t) - \nu(t)\| \leq \varepsilon_\nu, \quad (20)$$

$$R_2 : \|\tau_s(t) - \tau(t)\| \leq \varepsilon_\tau, \quad (21)$$

$$R_3 : \nu_s \text{ is transmitted to the controller.} \quad (22)$$

Specifically, with  $R_1$ ,  $R_2$  and  $R_3$  rules, the ASV sends its state data to the controller only when  $\bar{R}_1$  is satisfied. The  $i$ th time instant of the state data transmission is expressed by a monotonic sequence defined as  $\{s_i\}_{i=1}^\infty$  with  $s_i \in \mathbb{R}^+$ . With this triggered state data, the new uncertainties are approximated by the NNs, and the new control inputs of the ASV are computed by the controller using the presented saturated kinetic control law and the approximated uncertainties.

Likewise, the controller sends its new feedback control input data to the ASV only when  $\bar{R}_2 \wedge R_3$  is satisfied. The  $j$ th time instant of the control input data transmission is expressed by another monotonic sequence defined as  $\{r_j\}_{j=1}^\infty$  with  $r_j \in \mathbb{R}^+$ .

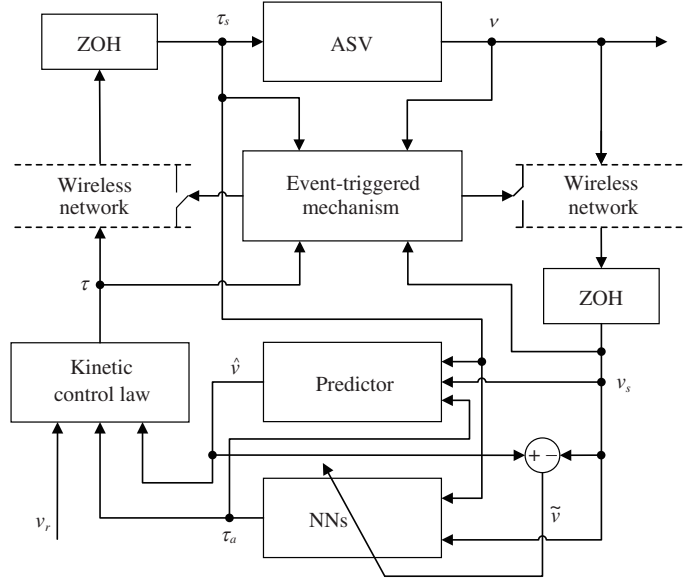


**Figure 2** Event-triggered NN kinetic control architecture.

### 3.4 Zero order holds

The designed event-triggered NN control structure is shown in Figure 2. ZOHs are applied to store the previous transmitted signal till the next event is triggered. The ZOHs in this paper work in the following way.

Let  $z(t)$  denote the current signal before transmitted and  $z_s(t_i)$  denote the last signal held by the ZOH in  $t \in (t_i, t_{i+1})$ , where  $i = 1, \dots, n$ . Once an event is triggered at  $t = t_{i+1}$ , the event-triggered mechanism allows the current signal  $z(t_{i+1})$  to be transmitted through the wireless network. Once receiving  $z(t)$ , the last signal  $z_s(t_i)$  held by the ZOH is replaced by  $z(t_{i+1})$ . Then  $z(t_{i+1})$  is held till the next event triggered.

## 4 Stability and Zeno behavior analysis

In this section, the Zeno behavior and stability of the closed-loop system are analyzed. The closed-loop system can be viewed as a system cascaded by the estimation error subsystem (14) and the velocity tracking error subsystem (17). Firstly, the stability of the subsystem (14) is presented.

**Lemma 1.** The subsystem (14), regarded as a system with states being  $\tilde{v}$ ,  $\tilde{W}_u$ ,  $\tilde{W}_v$  and  $\tilde{W}_r$ , inputs being  $\tilde{v}_e$ ,  $\varepsilon_e$ ,  $\tilde{W}_u$ ,  $\tilde{W}_r$  and  $\tilde{W}_v$ , is input-to-state stable.

*Proof.* Define a Lyapunov function  $V_1$  as

$$V_1 = \frac{1}{2} \left\{ \tilde{v}^T M \tilde{v} + \tilde{W}_u^T \Gamma_u^{-1} \tilde{W}_u + \tilde{W}_v^T \Gamma_v^{-1} \tilde{W}_v + \tilde{W}_r^T \Gamma_r^{-1} \tilde{W}_r \right\}. \quad (23)$$

Taking the time derivative and using (14),  $\dot{V}_1$  is given by

$$\dot{V}_1 = -\tilde{v}^T F \tilde{v} - \tilde{v}^T F \tilde{v}_e - \tilde{v}^T \varepsilon_e - \tilde{W}_u^T \beta(\vartheta_{us}) \tilde{u}_e - \tilde{W}_v^T \beta(\vartheta_{vs}) \tilde{v}_e - \tilde{W}_r^T \beta(\vartheta_{rs}) \tilde{r}_e. \quad (24)$$

It satisfies

$$\begin{aligned} \dot{V}_1 &\leq -\lambda_{\min}(F) \|\tilde{v}\|^2 - \lambda_{\min}(F) \|\tilde{W}_u\|^2 - \lambda_{\min}(F) \|\tilde{W}_v\|^2 - \lambda_{\min}(F) \|\tilde{W}_r\|^2 + \lambda_{\max}(F) \|\tilde{v}\| \|\tilde{v}_e\| \\ &\quad + \|\tilde{v}\| \|\varepsilon_e\| + \|\tilde{W}_u\| \|\beta(\vartheta_{us})\| \|\tilde{u}_e\| + \lambda_{\min}(F) \|\tilde{W}_u\|^2 + \|\tilde{W}_v\| \|\beta(\vartheta_{vs})\| \|\tilde{v}_e\| + \lambda_{\min}(F) \|\tilde{W}_v\|^2 \\ &\quad + \|\tilde{W}_r\| \|\beta(\vartheta_{rs})\| \|\tilde{r}_e\| + \lambda_{\min}(F) \|\tilde{W}_r\|^2 \\ &\leq -\lambda_{\min}(F) \|E_1\|^2 + \|h_1\| \|E_1\|, \end{aligned} \quad (25)$$

where  $E_1 = [\|\tilde{v}\|, \|\tilde{W}_u\|, \|\tilde{W}_v\|, \|\tilde{W}_r\|]^T$  and  $h_1 = [\lambda_{\max}(F)\|\tilde{v}_e\| + \|\varepsilon_e\|, \|\beta(\vartheta_{us})\|\|\tilde{u}_e\| + \lambda_{\min}(F)\|\tilde{W}_u\|, \|\beta(\vartheta_{vs})\|\|\tilde{v}_e\| + \lambda_{\min}(F)\|\tilde{W}_v\|, \|\beta(\vartheta_{rs})\|\|\tilde{r}_e\| + \lambda_{\min}(F)\|\tilde{W}_r\|]^T$ .

Because

$$\begin{aligned} \|E_1\| &\geq \frac{\lambda_{\max}(F)\|\tilde{v}_e\|}{\theta_1\lambda_{\min}(F)} + \frac{\|\varepsilon_e\|}{\theta_1\lambda_{\min}(F)} + \frac{\|\beta(\vartheta_{us})\|\|\tilde{u}_e\|}{\theta_1\lambda_{\min}(F)} + \frac{\|\tilde{W}_u\|}{\theta_1} + \frac{\|\beta(\vartheta_{vs})\|\|\tilde{v}_e\|}{\theta_1\lambda_{\min}(F)} + \frac{\|\tilde{W}_v\|}{\theta_1} \\ &\quad + \frac{\|\beta(\vartheta_{rs})\|\|\tilde{r}_e\|}{\theta_1\lambda_{\min}(F)} + \frac{\|\tilde{W}_r\|}{\theta_1} \\ &\geq \frac{\|h_1\|}{\theta_1\lambda_{\min}(F)}, \end{aligned} \tag{26}$$

it renders

$$\dot{V}_1 \leq -(1 - \theta_1)\lambda_{\min}(F)\|E_1\|^2, \tag{27}$$

where  $0 < \theta_1 < 1$ .

As a result, the subsystem (14) is input-to-state stable, and

$$\begin{aligned} \|E_1(t)\| &\leq \max\{\varpi_1(\|E_1(0)\|, t), \kappa_1(\|\tilde{v}_e\|) + \kappa_2(\|\varepsilon_e\|) + \kappa_3(\|\tilde{u}_e\|) + \kappa_4(\|\tilde{W}_u\|) + \kappa_5(\|\tilde{v}_e\|) \\ &\quad + \kappa_6(\|\tilde{W}_v\|) + \kappa_7(\|\tilde{r}_e\|) + \kappa_8(\|\tilde{W}_r\|)\}, \end{aligned} \tag{28}$$

where  $\varpi_1(\cdot)$  denotes a  $\mathcal{KL}$  function;  $\kappa_1(\cdot)$ ,  $\kappa_2(\cdot)$ ,  $\kappa_3(\cdot)$ ,  $\kappa_4(\cdot)$ ,  $\kappa_5(\cdot)$ ,  $\kappa_6(\cdot)$ ,  $\kappa_7(\cdot)$  and  $\kappa_8(\cdot)$  denote  $\mathcal{K}$  functions as follows:

$$\left\{ \begin{aligned} \kappa_1(s) &= \sqrt{\frac{\lambda_{\max}(S_1)}{\lambda_{\min}(S_1)} \frac{\lambda_{\max}(F)s}{\theta_1\lambda_{\min}(F)}}, \\ \kappa_2(s) &= \sqrt{\frac{\lambda_{\max}(S_1)}{\lambda_{\min}(S_1)} \frac{s}{\theta_1\lambda_{\min}(F)}}, \\ \kappa_3(s) &= \sqrt{\frac{\lambda_{\max}(S_1)}{\lambda_{\min}(S_1)} \frac{\|\beta(\vartheta_{us})\|s}{\theta_1\lambda_{\min}(F)}}, \\ \kappa_4(s) &= \sqrt{\frac{\lambda_{\max}(S_1)}{\lambda_{\min}(S_1)} \frac{s}{\theta_1}}, \\ \kappa_5(s) &= \sqrt{\frac{\lambda_{\max}(S_1)}{\lambda_{\min}(S_1)} \frac{\|\beta(\vartheta_{vs})\|s}{\theta_1\lambda_{\min}(F)}}, \\ \kappa_6(s) &= \sqrt{\frac{\lambda_{\max}(S_1)}{\lambda_{\min}(S_1)} \frac{s}{\theta_1}}, \\ \kappa_7(s) &= \sqrt{\frac{\lambda_{\max}(S_1)}{\lambda_{\min}(S_1)} \frac{\|\beta(\vartheta_{rs})\|s}{\theta_1\lambda_{\min}(F)}}, \\ \kappa_8(s) &= \sqrt{\frac{\lambda_{\max}(S_1)}{\lambda_{\min}(S_1)} \frac{s}{\theta_1}}, \end{aligned} \right. \tag{29}$$

with  $S_1 = \text{diag}\{M, \Gamma_u^{-1}, \Gamma_v^{-1}, \Gamma_r^{-1}\}$ .

The projection operation [38] guarantees the boundness of  $\tilde{W}$ . Besides, the upper bounds are

$$\left\{ \begin{aligned} \|\tilde{W}_u\| &\leq 2W_u^* + \epsilon_1, \\ \|\tilde{W}_v\| &\leq 2W_v^* + \epsilon_2, \\ \|\tilde{W}_r\| &\leq 2W_r^* + \epsilon_3. \end{aligned} \right. \tag{30}$$

The stability of the velocity tracking error subsystem (17) is analyzed then.

**Lemma 2.** The subsystem (17), regarded as a system with the state being  $\hat{e}$ , inputs being  $\tilde{\tau}_e$ ,  $\tilde{\nu}$  and  $\tilde{\nu}_e$ , is input-to-state stable.

*Proof.* Define a Lyapunov function as

$$V_2 = \frac{1}{2} \hat{e}^T M \hat{e}. \tag{31}$$

Using (17), the time derivation of  $\dot{V}_2$  is developed as

$$\dot{V}_2 = - \frac{\hat{e}^T M \hat{e}}{\sqrt{\|\hat{e}\|^2 + \Delta^2}} - \hat{e}^T \tilde{\tau}_e - \hat{e}^T F \tilde{\nu} - \hat{e}^T F \tilde{\nu}_e. \tag{32}$$

It satisfies

$$\begin{aligned} \dot{V}_2 &\leq -\lambda_{\min}(K) \frac{\|\hat{e}\|^2}{\sqrt{\|\hat{e}\|^2 + \Delta^2}} + \|\hat{e}\| \|\tilde{\tau}_e\| + \lambda_{\max}(F) \|\hat{e}\| \|\tilde{\nu}\| + \lambda_{\max}(F) \|\hat{e}\| \|\tilde{\nu}_e\| \\ &\leq -\frac{\lambda_{\min}(K) \|E_2\|^2}{\sqrt{\|E_2\|^2 + \Delta^2}} + \|h_2\| \|E_2\|, \end{aligned} \tag{33}$$

where  $E_2 = \hat{e}$ ,  $h_2 = [\|\tilde{\tau}_e\|, \lambda_{\max}(F) \|\tilde{\nu}\|, \lambda_{\max}(F) \|\tilde{\nu}_e\|]^T$ .

Noting that

$$\begin{aligned} \frac{\|E_2\|}{\sqrt{\|E_2\|^2 + \Delta^2}} &\geq \frac{\|\tilde{\tau}_e\|}{\theta_2 \lambda_{\min}(K)} + \frac{\lambda_{\max}(F) \|\tilde{\nu}\|}{\theta_2 \lambda_{\min}(K)} + \frac{\lambda_{\max}(F) \|\tilde{\nu}_e\|}{\theta_2 \lambda_{\min}(K)} \\ &\geq \frac{\|h_2\|}{\theta_2 \lambda_{\min}(K)}, \end{aligned} \tag{34}$$

it renders

$$\dot{V}_2 \leq -(1 - \theta_2) \lambda_{\min}(K) \frac{\|E_2\|^2}{\sqrt{\|E_2\|^2 + \Delta^2}}, \tag{35}$$

where  $0 < \theta_2 < 1$ .

It renders that subsystem (17) is input-to-state stable, and

$$\|E_2(t)\| \leq \max\{\varpi_2(\|E_2(0)\|, t), \kappa_9(\|\tilde{\tau}_e\|), \kappa_{10}(\|\tilde{\nu}\|), \kappa_{11}(\|\tilde{\nu}_e\|)\}, \tag{36}$$

where  $\varpi_2$  is a  $\mathcal{KL}$  function;  $\kappa_9(\cdot)$ ,  $\kappa_{10}(\cdot)$  and  $\kappa_{11}(\cdot)$  denote  $\mathcal{K}$  functions as follows:

$$\begin{cases} \kappa_9(s) = \mu^{-1} \left( \sqrt{\frac{\lambda_{\max}(M)}{\lambda_{\min}(M)}} \frac{s}{\theta_2 \lambda_{\min}(K)} \right), \\ \kappa_{10}(s) = \mu^{-1} \left( \sqrt{\frac{\lambda_{\max}(M)}{\lambda_{\min}(M)}} \frac{\lambda_{\max}(F) s}{\theta_2 \lambda_{\min}(K)} \right), \\ \kappa_{11}(s) = \mu^{-1} \left( \sqrt{\frac{\lambda_{\max}(M)}{\lambda_{\min}(M)}} \frac{\lambda_{\max}(F) s}{\theta_2 \lambda_{\min}(K)} \right), \end{cases} \tag{37}$$

with  $\mu(s) = s^2 / \sqrt{s^2 + \Delta^2}$ .

The stability of the system cascaded by (14) and (17) is presented as the following theorem.

**Theorem 1.** Considering the ASV kinetics being (6), the controller formed by (8), (11), (12), (16), and the event-triggered rules being (20)–(22), the resulting closed-loop system cascaded by (14) and (17) is input-to-state stable. Moreover, the errors  $e$  and  $\hat{e}$  are uniformly ultimately bounded.

*Proof.* From the user-defined event-triggered rules, it renders  $\|\tilde{\nu}_e\| \leq \varepsilon_\nu$  and  $\|\tilde{\tau}_e\| \leq \varepsilon_\tau$ . It can be obtained from Lemmas 1 and 2 that: subsystem (14) with states being  $\tilde{\nu}$ ,  $\tilde{W}_u$ ,  $\tilde{W}_v$ ,  $\tilde{W}_r$  and inputs being  $\tilde{\nu}_e$ ,  $\varepsilon_e$ ,  $\tilde{W}_u$ ,  $\tilde{W}_v$ ,  $\tilde{W}_r$  is input-to-state stable; subsystem (17) with state being  $\hat{e}$  and inputs being  $\tilde{\tau}_e$ ,  $\tilde{\nu}$ ,  $\tilde{\nu}_e$

is input-to-state stable. By Lemma C.4 [39], the cascade system with states being  $\tilde{\nu}$ ,  $\tilde{W}_u$ ,  $\tilde{W}_v$ ,  $\tilde{W}_r$  and inputs being  $\tilde{\nu}_e$ ,  $\varepsilon_e$ ,  $\tilde{W}_u$ ,  $\tilde{W}_v$ ,  $\tilde{W}_r$ ,  $\tilde{\tau}_e$  is input-to-state stable. Hence, there exist a  $\mathcal{KL}$  function  $\varpi$  and a  $\mathcal{K}$  function  $\kappa$ , such that

$$\|E(t)\| \leq \varpi(\|E(0)\|, t) + \kappa(\|\tilde{\nu}_e, \varepsilon_e, \tilde{W}_u, \tilde{W}_v, \tilde{W}_r, \tilde{\tau}_e\|), \tag{38}$$

where  $E = [\tilde{\nu}, \tilde{W}_u, \tilde{W}_v, \tilde{W}_r, \hat{e}]^T$ . Note that  $\tilde{\nu}_e$ ,  $\varepsilon_e$ ,  $\tilde{W}_u$ ,  $\tilde{W}_v$ ,  $\tilde{W}_r$  and  $\tilde{\tau}_e$  are bounded by  $\varepsilon_\nu$ ,  $\varepsilon_e^*$ ,  $2W_u^* + \varepsilon_1$ ,  $2W_v^* + \varepsilon_2$ ,  $2W_r^* + \varepsilon_3$  and  $\varepsilon_\tau$ , respectively. Then, the errors  $\tilde{\nu}$ ,  $\tilde{W}_u$ ,  $\tilde{W}_v$ ,  $\tilde{W}_r$  and  $\hat{e}$  are all bounded.

Besides, because

$$\|e\| = \|\tilde{\nu} + \hat{e}\| \leq \|\hat{e}\| + \|\tilde{\nu}\|, \tag{39}$$

the velocity tracking error  $e$  is uniformly ultimately bounded. The proof is completed.

Theorem 2 shows that there exist positive lower bounds for the least inter-event time, and it means the Zeno behavior does not happen in the proposed event-triggered NN control method.

Let  $r_m^i \in (s_i, s_{i+1})$  be the  $m$ th time instant when  $\bar{R}_2$  is satisfied over  $(s_i, s_{i+1})$  similarly to [27]. Because  $\{s_i\}_{i=1}^\infty$  is a subsequence of  $\{r_j\}_{j=1}^\infty$ , then  $\{r_j\}_{j=1}^\infty = \{s_i\}_{i=1}^\infty \cup \{r_m^i\}_{i=1, m=1}^{\infty, n_i}$  holds, where  $n_i \in \mathbb{N}$  denotes the number of violation times for  $\bar{R}_2$  over  $(s_i, s_{i+1})$ .

**Theorem 2.** Consider the ASV kinetics given by (6), the saturated kinetic control law given by (16), the estimator given by (11), the NN given by (8), the NN weights update law given by (12) and the event-triggered rules given by (20)–(22). Let the ASV states be transmitted to the controller taking place when  $\bar{R}_1$  is satisfied. Let the control inputs be transmitted to the ASV taking place when  $\bar{R}_2 \wedge \bar{R}_3$  is satisfied. Then, there exist positive scalars  $\alpha_\nu = \varepsilon_\nu/\bar{h}_\nu$  and  $\alpha_\tau = \varepsilon_\tau/\bar{h}_\tau$  such that

$$s_{i+1} - s_i \geq \alpha_\nu, \quad \forall i \in \mathbb{N}, \tag{40}$$

$$r_{j+1}^i - r_j^i \geq \alpha_\tau, \quad \forall j \in \{0, \dots, m_i\}, \quad \forall i \in \mathbb{N}, \tag{41}$$

where

$$\bar{h}_\nu \geq \frac{\|\tau_s\| + \|f(\cdot)\|}{\lambda_{\min}(M)}, \tag{42}$$

$$\bar{h}_\tau \geq \frac{\lambda_{\max}(K)}{\sqrt{\|\hat{e}\|^2 + \Delta^2}} (\|\dot{\hat{e}}\| + \|\hat{e}\|^2) + \|\dot{\tau}_a\|. \tag{43}$$

*Proof.* The time derivation of  $\|\nu_s(t) - \nu(t)\|$ ,  $t \in (s_i, s_{i+1})$ ,  $\forall i \in \mathbb{N}$  is developed as

$$\begin{aligned} \frac{d}{dt} \|\nu_s(t) - \nu(t)\| &\leq \|\dot{\nu}_s(t) - \dot{\nu}(t)\| = \|\dot{\nu}(t)\| \\ &\leq \frac{\|\tau_s\| + \|f(\cdot)\|}{\lambda_{\min}(M)}. \end{aligned} \tag{44}$$

By Theorem 1, the entire closed-loop system is input-to-state stable. Therefore, there is an upper bound for (44). The upper bound is denoted as  $\bar{h}_\nu$ . With the initial condition of the event-trigger satisfying

$$\lim_{t \rightarrow s_i^+} \|\nu_s(t) - \nu(t)\| = 0, \tag{45}$$

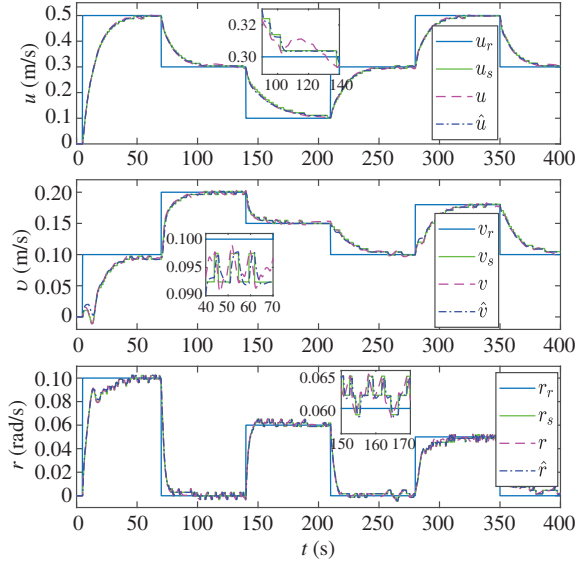
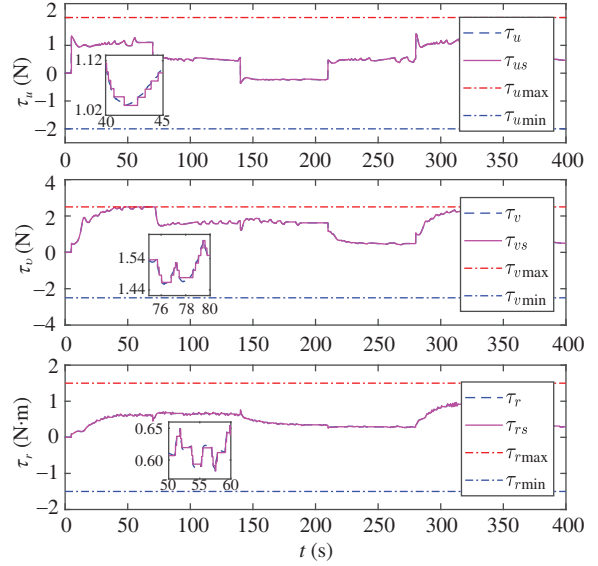
one can get from (44) that

$$\|\nu_s(t) - \nu(t)\| \leq \int_{s_i}^t \bar{h}_\nu d\ell = \bar{h}_\nu(t - s_i). \tag{46}$$

When  $\bar{R}_1$  is satisfied, it renders  $\lim_{t \rightarrow s_{i+1}^-} \|\nu_s(t) - \nu(t)\| = \varepsilon_\nu$ , and it follows from (46) that  $s_{i+1} - s_i \geq \alpha_\nu$ .

Similarly, the time derivation of  $\|\tau_s(t) - \tau(t)\|$ ,  $t \in (r_j^i, r_{j+1}^i)$ ,  $\forall j \in \mathbb{N}$  is developed as

$$\frac{d}{dt} \|\tau_s(t) - \tau(t)\| \leq \|\dot{\tau}_s(t) - \dot{\tau}(t)\| = \|\dot{\tau}(t)\|$$


**Figure 3** (Color online) Command tracking performance.

**Figure 4** (Color online) Control inputs.

$$\leq \frac{\lambda_{\max}(K)}{\sqrt{\|\hat{e}\|^2 + \Delta^2}} (\|\dot{e}\| + \|\hat{e}\|^2) + \|\dot{\tau}_a\|. \quad (47)$$

By Theorem 1, the entire closed-loop system is input-to-state stable. Therefore, there is an upper bound for (47). The upper bound is denoted as  $\bar{h}_\tau$ . With the initial condition of the event-trigger satisfying

$$\lim_{t \rightarrow r_j^{i+}} \|\tau_s(t) - \tau(t)\| = 0, \quad (48)$$

one can get from (47) that

$$\|\tau_s(t) - \tau(t)\| \leq \int_{r_j^i}^t \bar{h}_\tau dt = \bar{h}_\tau(t - r_j^i). \quad (49)$$

When  $\bar{R}_2 \wedge R_3$  is satisfied, it renders  $\lim_{t \rightarrow r_{j+1}^i} \|\tau_s(t) - \tau(t)\| = \varepsilon_\tau$ , and it follows from (49) that  $r_{j+1}^i - r_j^i \geq \alpha_\tau$ .

## 5 Simulation example

In the simulation section, an example is provided to evaluate the effectiveness of the presented event-triggered NN control approach.

Let an ASV in [22] follow a time-varying speed command  $\nu_r \in \mathbb{R}^3$ . The parameters of the ASV are  $m_{11} = 25.79$ ,  $m_{22} = 33.81$ ,  $m_{23} = m_{32} = 1.095$ ,  $m_{33} = 2.75$ ,  $d_{11} = 0.713 + 5.64u^2 + 1.24|u|$ ,  $d_{22} = 0.8765 + 37.1|v| + 0.811|r|$ ,  $d_{33} = 1.87 - 0.079|v| + 0.746|r|$ ,  $d_{23} = 7.16 + 0.851|v| + 3.38|r|$ , and  $d_{32} = 0.0324 + 3.88|v| + 0.129|r|$ . The activation function  $\beta(\rho)$  of NN is chosen as  $\beta(\rho) = (1 - e^{-\rho}) / (1 + e^{-\rho})$ .

The controller parameters are chosen as  $\Gamma_u = 3.5$ ,  $\Gamma_v = 5$ ,  $\Gamma_r = 20$ ,  $\Delta = 1$ ,  $k_1 = 20$ ,  $k_2 = 40$ ,  $k_3 = 10$ ,  $k_4 = 3$ ,  $k_5 = 5$ ,  $k_6 = 1$ ,  $\varepsilon_{\nu u} = 0.01$ ,  $\varepsilon_{\nu v} = 0.005$ ,  $\varepsilon_{\nu r} = 0.003$ ,  $\varepsilon_{\tau u} = 0.01$ ,  $\varepsilon_{\tau v} = 0.008$ ,  $\varepsilon_{\tau r} = 0.008$ , and  $t_p^* = 0.01$ .

Simulation results are afforded from Figures 3–9. The speed commands following performance is drawn in Figure 3. The speed commands are well followed although the ASV suffers from uncertain dynamics and unknown kinetics. The vehicle states are estimated effectively by the predictor with aperiodic sampling of data and the estimated uncertainties. The control inputs of the ASV are drawn in Figure 4. It

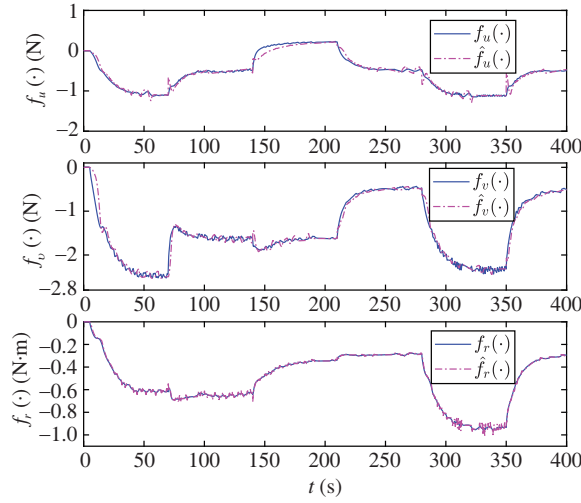


**Figure 5** (Color online) Approximation of uncertainties by NNs.

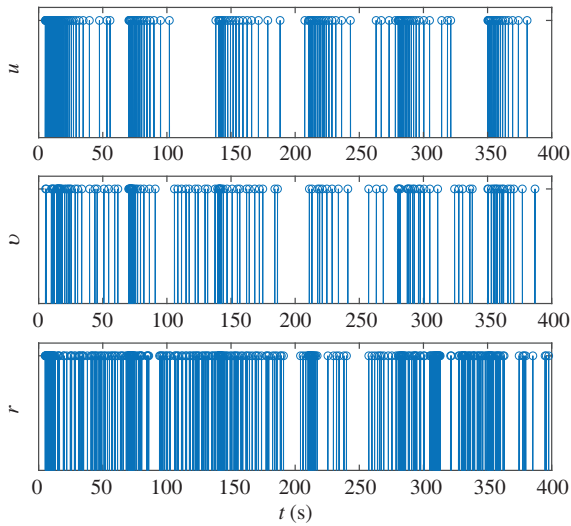


**Figure 6** (Color online) Events caused by the sampling of vehicle states.

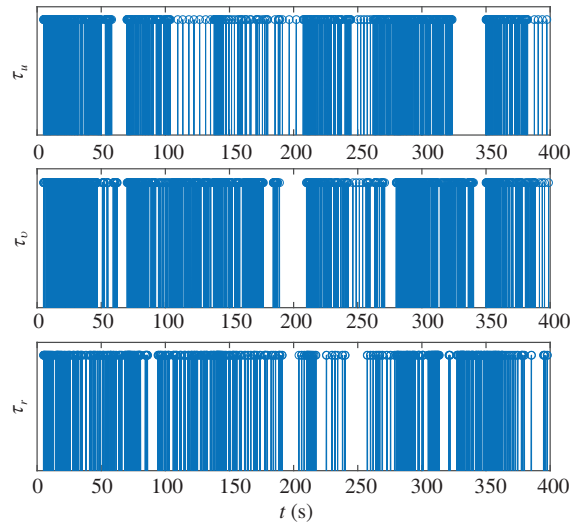


**Figure 7** (Color online) Events caused by the updating of control inputs.

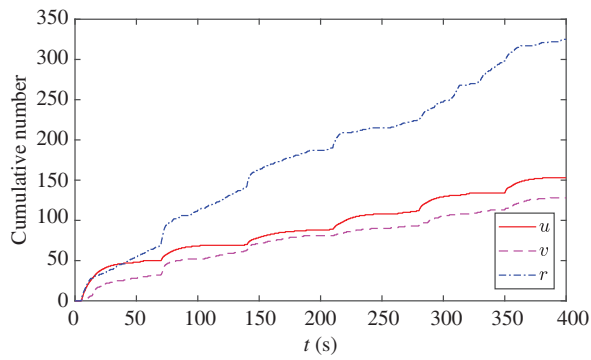


**Figure 8** (Color online) Event-triggered times caused by the sampling of vehicle states.

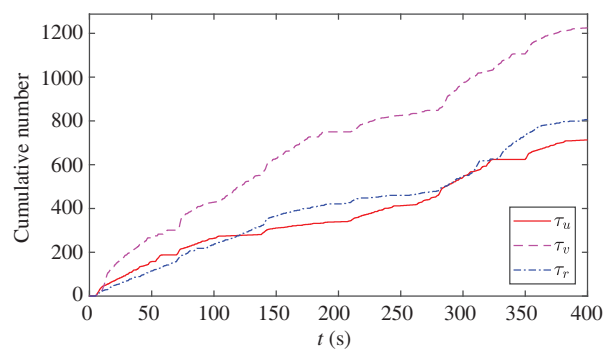


**Figure 9** (Color online) Event-triggered times caused by the updating of control inputs.

demonstrates that the control inputs are bounded within 2 N, 2.5 N and 1.5 Nm, respectively. The uncertainties and the outputs of NNs are drawn in Figure 5. The uncertainties are efficiently approached

by the NNs via aperiodic sampling of data. Figure 6 shows the events caused by the sampling of the vehicle states. Figure 7 shows the events caused by the updating of control inputs. It can be observed from Figures 6 and 7 that data transmissions are aperiodic. Moreover, there are many moments that no events are triggered. Therefore, no data need to be transmitted over wireless network. Figure 8 shows the triggered cumulative times of the vehicle states. Figure 9 shows the triggered cumulative times of the control inputs. The cumulative times of  $u$ ,  $v$ ,  $r$ ,  $\tau_u$ ,  $\tau_v$  and  $\tau_r$  are 153, 128, 325, 713, 1225 and 806, respectively. Compared with the time-triggered system (the sample period is 0.01 s), which the trigger cumulative times are 40000 for both vehicle states and control inputs, the trigger cumulative times are reduced 96.9% at least, and it demonstrates that the developed event-triggered NN control method can reduce the network traffic.

## 6 Conclusion

This paper presents an event-triggered NN control method for ASVs over wireless network. The uncertainties are approximated efficiently by the NNs via aperiodic sampling of vehicle states. The bounded kinetic control law is developed based on a saturation function and NNs. The event-triggered mechanism is employed to reduce the network traffic. The two-way data transmissions are determined by the event-triggered mechanism. The closed-loop system is proved to be input-to-state stable via cascade stability analysis, and all error signals are proved to be uniformly ultimately bounded. Zeno behavior is proved to be excluded. Simulation results show that the trigger times are reduced and the system stability and speed following performance are guaranteed by using the proposed event-triggered NN control method.

**Acknowledgements** This work was supported in part by National Natural Science Foundation of China (Grant Nos. 61673081, 51979020, 51909021, 51579023), Training Program for High-level Technical Talent in Transportation Industry (Grant No. 2018-030), Innovative Talents in Universities of Liaoning Province (Grant No. LR2017014), Science and Technology Fund for Distinguished Young Scholars of Dalian (Grant No. 2018RJ08), Stable Supporting Fund of Science and Technology on Underwater Vehicle Technology (Grant No. JCKYS2019604SXJQR-01), Fundamental Research Funds for the Central Universities (Grant No. 3132019319), and China Postdoctoral Science Foundation (Grant No. 2019M650086).

## References

- 1 Fossen T I. Handbook of marine craft hydrodynamics and motion control. *IEEE Control Syst*, 2016, 36: 78–79
- 2 Tee K P, Ge S S. Control of fully actuated ocean surface vessels using a class of feedforward approximators. *IEEE Trans Contr Syst Technol*, 2006, 14: 750–756
- 3 Liu L, Wang D, Peng Z H, et al. Saturated coordinated control of multiple underactuated unmanned surface vehicles over a closed curve. *Sci China Inf Sci*, 2017, 60: 070203
- 4 Dai S L, He S D, Lin H, et al. Platoon formation control with prescribed performance guarantees for USVs. *IEEE Trans Ind Electron*, 2018, 65: 4237–4246
- 5 Peng Z H, Wang D, Li T S. Predictor-based neural dynamic surface control for distributed formation tracking of multiple marine surface vehicles with improved transient performance. *Sci China Inf Sci*, 2016, 59: 092210
- 6 Hovakimyan N, Nardi F, Calise A, et al. Adaptive output feedback control of uncertain nonlinear systems using single-hidden-layer neural networks. *IEEE Trans Neural Netw*, 2002, 13: 1420–1431
- 7 Peng Z H, Wang J, Wang D. Distributed containment maneuvering of multiple marine vessels via neurodynamics-based output feedback. *IEEE Trans Ind Electron*, 2017, 64: 3831–3839
- 8 Dai S L, Wang M, Wang C, et al. Learning from adaptive neural network output feedback control of uncertain ocean surface ship dynamics. *Int J Adapt Control Signal Process*, 2014, 28: 341–365
- 9 Dai S L, He S D, Wang M, et al. Adaptive neural control of underactuated surface vessels with prescribed performance guarantees. *IEEE Trans Neural Netw Learn Syst*, 2018. doi: 10.1109/TNNLS.2018.2876685
- 10 Zhao Z, He W, Ge S S. Adaptive neural network control of a fully actuated marine surface vessel with multiple output constraints. *IEEE Trans Contr Syst Technol*, 2014, 22: 1536–1543
- 11 Abdelatti M, Yuan C Z, Zeng W, et al. Cooperative deterministic learning control for a group of homogeneous nonlinear uncertain robot manipulators. *Sci China Inf Sci*, 2018, 61: 112201
- 12 Peng Z H, Wang D, Wang J. Cooperative dynamic positioning of multiple marine offshore vessels: a modular design. *IEEE/ASME Trans Mechatron*, 2016, 21: 1210–1221
- 13 Zheng Z, Feroskhan M. Path following of a surface vessel with prescribed performance in the presence of input saturation and external disturbances. *IEEE/ASME Trans Mechatron*, 2017, 22: 2564–2575
- 14 Peng Z H, Wang J, Han Q L. Path-following control of autonomous underwater vehicles subject to velocity and input constraints via neurodynamic optimization. *IEEE Trans Ind Electron*, 2019, 66: 8724–8732

- 15 Xia R S, Wu Q X, Chen M. Disturbance observer-based optimal longitudinal trajectory control of near space vehicle. *Sci China Inf Sci*, 2019, 62: 050212
- 16 Ashrafiuon H, Muske K R, McNinch L C, et al. Sliding-mode tracking control of surface vessels. *IEEE Trans Ind Electron*, 2008, 55: 4004–4012
- 17 Cui R X, Zhang X, Cui D. Adaptive sliding-mode attitude control for autonomous underwater vehicles with input nonlinearities. *Ocean Eng*, 2016, 123: 45–54
- 18 Xiang X B, Liu C, Su H S, et al. On decentralized adaptive full-order sliding mode control of multiple UAVs. *ISA Trans*, 2017, 71: 196–205
- 19 Yang Y S, Zhou C J, Ren J S. Model reference adaptive robust fuzzy control for ship steering autopilot with uncertain nonlinear systems. *Appl Soft Comput*, 2003, 3: 305–316
- 20 Xiang X B, Yu C Y, Zhang Q. Robust fuzzy 3D path following for autonomous underwater vehicle subject to uncertainties. *Comput Oper Res*, 2017, 84: 165–177
- 21 Chen Z Y, Huang J. Attitude tracking and disturbance rejection of rigid spacecraft by adaptive control. *IEEE Trans Automat Contr*, 2009, 54: 600–605
- 22 Skjetne R, Fossen T I, Kokotović P V. Adaptive maneuvering, with experiments, for a model ship in a marine control laboratory. *Automatica*, 2005, 41: 289–298
- 23 Qin H D, Chen H, Sun Y C, et al. The distributed adaptive finite-time chattering reduction containment control for multiple ocean bottom flying nodes. *Int J Fuzzy Syst*, 2019, 21: 607–619
- 24 Chen Z Y. A novel adaptive control approach for nonlinearly parameterized systems. *Int J Adapt Control Signal Process*, 2015, 29: 81–98
- 25 Albattat A, Gruenwald B, Yucelen T. Design and analysis of adaptive control systems over wireless networks. *J Dynamic Syst Measurement Control*, 2017, 139: 074501
- 26 Sahoo A, Xu H, Jagannathan S. Neural network-based event-triggered state feedback control of nonlinear continuous-time systems. *IEEE Trans Neural Netw Learn Syst*, 2016, 27: 497–509
- 27 Albattat A, Gruenwald B C, Yucelen T. On event-triggered adaptive architectures for decentralized and distributed control of large-scale modular systems. *Sensors*, 2016, 16: 1297
- 28 Li H P, Shi Y. Event-triggered robust model predictive control of continuous-time nonlinear systems. *Automatica*, 2014, 50: 1507–1513
- 29 Heemels W P M H, Donkers M C F. Model-based periodic event-triggered control for linear systems. *Automatica*, 2013, 49: 698–711
- 30 Xu W Y, Wang Z D, Ho D W C. Finite-horizon  $H_\infty$  consensus for multiagent systems with redundant channels via an observer-type event-triggered scheme. *IEEE Trans Cybern*, 2018, 48: 1567–1576
- 31 Zhang Z Q, Hao F, Zhang L, et al. Consensus of linear multi-agent systems via event-triggered control. *Int J Control*, 2014, 87: 1243–1251
- 32 Xu W Y, Chen G R, Ho D W C. A layered event-triggered consensus scheme. *IEEE Trans Cybern*, 2017, 47: 2334–2340
- 33 Peng Z H, Wang J S, Wang J. Constrained control of autonomous underwater vehicles based on command optimization and disturbance estimation. *IEEE Trans Ind Electron*, 2019, 66: 3627–3635
- 34 Harmouche M, Laghrouche S, Chitour Y. Global tracking for underactuated ships with bounded feedback controllers. *Int J Control*, 2014, 47: 1–9
- 35 Wang H, Wang D, Peng Z H. Adaptive dynamic surface control for cooperative path following of marine surface vehicles with input saturation. *Nonlin Dyn*, 2014, 77: 107–117
- 36 Zheng Z W, Sun L. Error-constrained path-following control for a stratospheric airship with actuator saturation and disturbances. *Int J Syst Sci*, 2017, 48: 3504–3521
- 37 Zheng Z W, Huang Y T, Xie L H, et al. Adaptive trajectory tracking control of a fully actuated surface vessel with asymmetrically constrained input and output. *IEEE Trans Contr Syst Technol*, 2018, 26: 1851–1859
- 38 Lavretsky E, Gibson T E. Projection operator in adaptive systems. 2011. ArXiv: 1112.4232
- 39 Krstic M, Kokotovic P V, Kanellakopoulos I. *Nonlinear and Adaptive Control Design*. New York: John Wiley & Sons, 1995